Figure 6 shows the change of corona wind velocity in the X direction (when Y = 10.5 mm, it refers to the horizontal position of the discharge tip in the solution domain). It can be seen that the higher the absolute value of the discharge voltage, the larger the corona wind velocity in the horizontal direction, and the easier it is for the wind to attenuate. In addition, the corona wind speed was 0 at the tip of the corona pole, rising quickly to the peak value and then plummeting in the horizontal direction. This phenomenon was commonly seen at different voltages, and the reason is: the flow of corona wind occured in the corona area, whose changes in velocity triggered the velocity change in other positions; the larger the absolute value of the voltage, the larger the field strength, and the greater the electric field force exerted on the electric fluid, which in turn rendered the horizontal diffusion distance of charged particles small. As can be seen from Figure 2, the greater the absolute value of the voltage, the smaller the horizontal width of the high-wind-speed area.

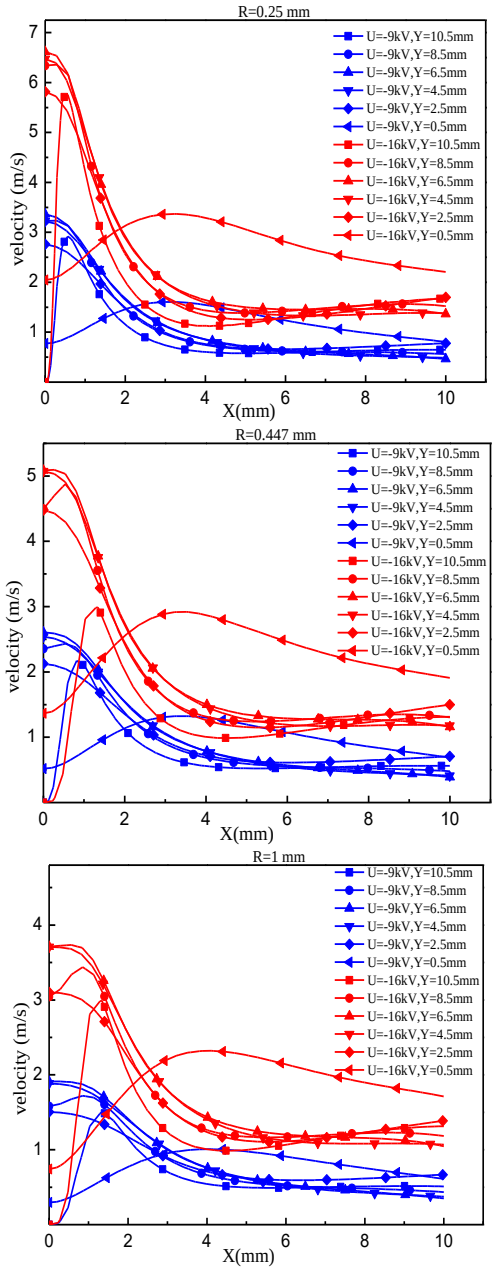

Figure 6. Corona wind velocity in X direction at different voltages

3.4 Influence of curvature radius on corona wind velocity

Figure 7 shows Y-direction corona wind velocities at different radii of curvature. As can be seen, the farther the corona wind is from the corona pole in the X direction, the faster the wind speed attenuates whatever the curvature radius. The fact that the smaller curvature radius corresponds to quicker attenuation, indicates that apart from discharge voltage, the radius of curvature also played a contributory factor to the width of the high-speed corona wind area. At various radii of curvature, velocities approach 0, both at the tip of the corona pile and near anode plates, albeit the difference of regional velocity between electrodes. This phenomenon shows that curvature radius only affects the speed of corona wind and the boundary of high-speed corona wind area, but is powerless with respect to other trends of change. In addition, when the X value was 3 mm and 4 mm, the stable region was shorter. This phenomenon is also reflected in Figure 5. It can be inferred from the cloud map of corona velocity in Figure 3 that the phenomenon resulted from the limiting of the corona area. In negative corona discharge, negative ions and electrons were generated at the tip of the discharge electrode. Because the tip had a relatively high field strength, the electric field force of these charged ions was greater and thereby the accelerating time was shorter. Meanwhile, these charged ions were moving vertically to the anode plate when they left the tip of the discharge electrode. Under the action of a strong electric field force, it was difficult for these ions to spread in the horizontal direction. Therefore, the high-speed corona wind area had arc-shaped boundaries and mainly lay inside the corona area. When the X value was 3 mm or 4 mm, the vertical sampling line passed through only a small portion of the high-speed area, leading to a shorter stable region at the location.

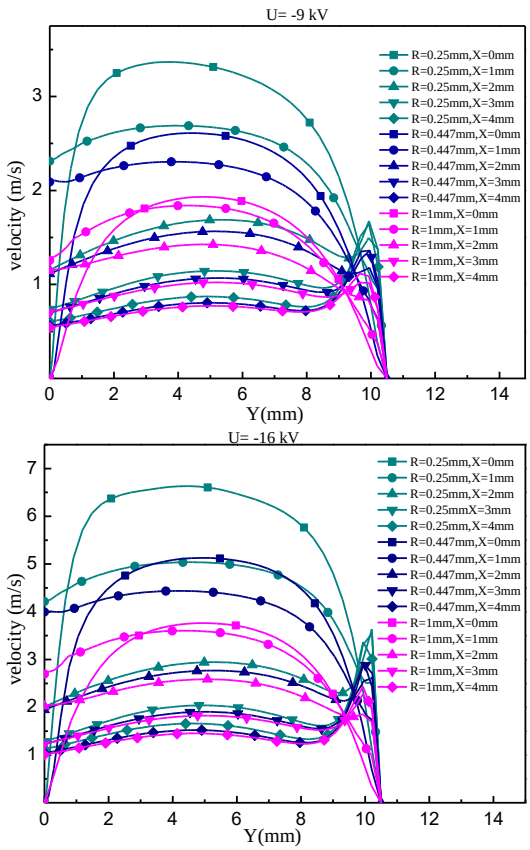

Figure 7. Y-direction corona wind velocity at different radii of curvature

Figure 8 shows the X-direction corona wind velocities at different radii of curvature. It was found that the smaller the radius of curvature, the larger the corona wind velocity in the area where the corona is facing the earth plate, and the faster the horizontal speed attenuation, which was reduced to a similar value in the end. In addition, when the curvature radius changed, the horizontal width of the high-wind-speed area also varied. By referring to the speed field in Figure 2, we summarized that the smaller the curvature radius, the narrower the fast-wind-speed area was horizontally. The two-dimensional asymmetrical solution domain used for calculation herein corresponds to the "spindle-like" high-speed corona wind area at the three-dimensional level. This area allowed negatively-charged particles to quickly leave the corona pole, increasing the probability of positively-charged particles to be neutralized. The neutral particles formed drifted towards the plate under the action of the corona wind, during which they could combine with electrons and be absorbed on the dust collector plate resultantly. Therefore, a rational design of corona pole layout can improve the near-corona dust environment by avoiding the clustering of massive dusts in the vicinity of the corona pole.

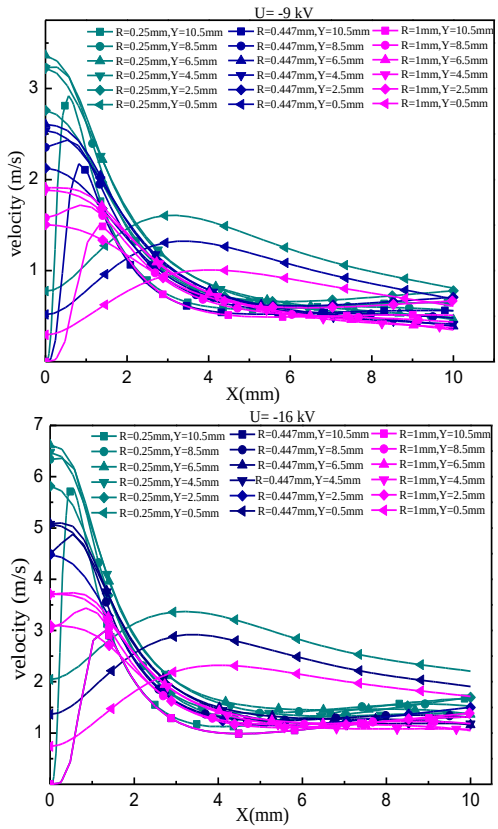

Figure 8. X-direction corona wind velocities at different radii of curvature

3. CONCLUSION

The research in this paper provides theoretical basis for the optimization of the flow field near the corona pole of ESP. The respective corona winds generated at a pair of voltages and three radiuses of curvature were simulated numerically. The main conclusions are:

1) The corona wind mainly forms in the corona area, and the change of the flow field in other locations is caused by the corona wind;

2) Under several corona voltages, all velocities of the corona wind within the corona area are accelerated first and then become stable, followed by reductions. At a fixed spatial position, the higher the absolute voltage value, the higher the corona wind velocity.

3) The change of curvature radius of the corona pole within the corona area contributes little to the stabilized area formed after the attenuation of corona wind. The smaller curvature radius results in a rise in the velocity of the corona wind and the axial width of the high-speed region, as well as the shrinkage of its overall horizontal width.

REFERENCES

[1] Yi Chengwu, Liu Shiwen, Shi Xuexin, et al., "Experiment study on the collection performance of single-stage double-vortex collecting plate electrostatic precipitator," *High Voltage Engineering*, vol. 42, no. 8, pp. 2651-2658, 2016.

[2] Li Xin, "The major causes and countermeasures that Influence the Performance parameters of electrical precipitator," Northeastern University, 2010.

[3] Pan Xiaohui, Cui Lin, Ma Chunyuan, "Influence of water film on the distribution and motion characteristics of fine particles in electrostatic precipitator," *Proceedings of the CSEE*. vol. 36, no. 16, pp. 4333-4342, 2016.

[4] Huang Bin, Yao Qiang, Li Shuiqing, et al., "Progress in technology of electrostatic enhancement for removal of PM2.5," *Power System Engineering*, vol. 19, no. 6, pp. 44-46, 2003.

[5] Liu Hao, Liu Shanghe, Cao Hefei, et al., "Experimental simulation system of corona discharges under high-altitude, low-pressure and low-temperature conditions," *High Voltage Engineering*, vol. 41, no. 2, pp. 578-583, 2015.

[6] Wang Liming, WAN Shuwei, Bian Xingming, et al., "Uitraviolet characteristics of negative dc corona discharge in extremely non-uniform electric field," *High Voltage Engineering*, vol. 40, no. 6, pp. 1614-1622, 2014.

[7] Yan Keping, Li Shuran, Feng Weiqiang, et al., "Analysis and prospect on key technology of high-voltage discharge for environmental engineering study and application." *High Voltage Engineering*, vol. 41, no. 8, pp.2528-2544, 2015.

[8] He Shoujie, Liu Shumin, Liu Zhiqiang, et al., "Simulation on the characteristics of a slotted hollow cathode discharge." *High Voltage Engineering*, vol. 41, no. 2, pp.516-522, 2015.

[9] Moreau E., "Airflow control by non-thermal plasma actuators," *Journal of Physics D: Applied Physics*, vol. 40, no. 3, pp. 605-636, 2007. DOI: 10.1-088/0022-3727/40/3/S01.

[10] Hinds W. C., *Aerosol Technology*, New York: John Wiley & Sons Inc, pp. 288-300, 1982.

[11] Shen Xinjun, Zeng Yuxuan, Zheng Qinzhen, et al., "Measurements of flow field in wire-plate electrostatic precipitator during positive or negative corona discharge using PIV Method," *High Voltage Engineering*, vol. 10, no. 9, pp. 2757-2763, 2014 .

[12] Nakamura H., Ohyama R., "An image analysis of positive ionic wind velocity under the DC corona discharge in needle-cylinder electrode system," I*EEE*

Conference on Electrical Insulation and Dielectric Phenomena, pp. 192-195, 2009. DOI: 1-0.1109/CEIDP.2009.5377857.

[13] Moreau E., Touchard G., "Enhancing the mechanical efficiency of electric wind in corona discharges," *Journal of Electrostatics*, vol. 66, no. 8, pp. 39-44, 2008.

[14] Yuan Junxiang, Qiu wei, Zheng Cheng, et al., "Study on characteristics of ionic wind from atmosphere discharge," *Proceedings of the CSEE*, vol. 29, no.13, pp. 110-116, 2009.

[15] Yuan Junxiang, Yang Lanjun, Zhang Qiaogen, et al., "Ionic wind characteristic of tine-plat affected by electrode parameter from atmosphere discharge," *Transactions of China Electrotechnical Society*, vol. 25, no. 1, pp. 24-29, 2010.

[16] Zeng Yuxuan. Shen Xinjun, Zhang Yuming, et al., "Experimental study of ionic wind in an electrostatic precipitatior," *Journal of Zhejiang University*, vol. 47, no. 12, pp. 2208-2211, 2013.

[17] Liang W J, Lin T. H., "The characteristics of ionic wind and its effect on electrostatic precipitator," *Aerosol Science and Technology*, vol. 20, no. 13, pp. 330-344, 1994.

[18] Gong Tao, Tang Fei, Wang Xiaohao, "Characteristics of ionicwind excited by multiple needles-net structure," *High Voltage Apparatus*, vol. 48, no. 5, pp. 33-36, 2012.

[19] Wang Wei, Yang Lanjun, Gao Jie, et al., "Experimental study on the thrust and the ratio of thrust to power of multi-points/grid ionic wind exciter," *Acta Phys Sin*, vol. 62, no.7, pp. 1-7, 2013.

[20] Li Qing, Li Haifeng, Sun Xiaorong, et al., "Experimental re-search and numerical simulation of electro-hydrodynamic incorona discharge," *High Voltage Engineering*, vol. 36, no. 11, pp. 2739-2744, 2010.

[21] Yang Lanjun, Wang Wei, Lin Cen, et al., "Experimental and theoretical research progress in ionic wind produced by corona discharge and its application," *High Voltage Engineering*, vol. 42, no. 2, pp. 1100-1108, 2016.

[22] Dong Sik Cho, Sangmo Kang, Yong Kweon Suh, et al., "Development of a bi-directional electrohydrodynamic pump: Parametric study with numerical simulation and flow visualization," *Advances in Mechanical Engineering*, vol. 8, no. 6, pp. 1–15, 2016. DOI: 10.1177/1687814016655777.

[23] Quentin Lancereau, Jean-Maxime Roux, Jean-Luc Achard, et al., "Electrohydrodynamic flow regimes in a cylindrical electrostatic precipitator," *IEEE Transactions on Dielectrics and Electrical Insulation*, vol. 20, no. 4, pp. 1409-1420, 2013.

[24] Rehena Nasrin, M. A. Alim, "Thermal performance of nanofluid filled solar flat plate collector," *International Journal of Heat and Technology*, vol. 33. no. 2, pp 17-24, 2015. DOI: 10.18280/ijht.330203.

[25] Yueping Qin, Song Kong, Wei Liu, et al., "Dimensionless analysis of the temperature field of surrounding rock in coalface with a finite volume method," *International Journal of Heat and Technology*, vol. 33, no. 3, pp 151-157, 2015. DOI: 10.18280/ijht.330323

[26] Fei-fei Wu, "Numerical simulation of Trichel pulse charateristics in bar-plate DC negative corona discharge," *Acta Physica Sinica*, vol. 11, pp. 338-347, 2013.

[27] Zhang Bailing, Wang Yutian, Li Yiwen, et al., "Numerical simulation and experimental study for low-pressure direct-current glow discharge," *High Voltage Engineering*, vol. 42, no. 3, pp. 724-730, 2016.